Bilateral equalization of synaptic output in olfactory glomeruli of Xenopus tadpoles

Marta Casas[1,2], Beatrice Terni[1,2] and Artur Llobet[1,2*]

[1] Laboratory of Neurobiology, Department of Pathology and Experimental Therapy, Institute of Neurosciences, University of Barcelona, 08907 L'Hospitalet de Llobregat, Barcelona, Spain

[2] Bellvitge Biomedical Research Institute (IDIBELL), 08907 L'Hospitalet de Llobregat, Barcelona, Spain

* Corresponding Author:
Artur Llobet
Laboratory of Neurobiology
Department of Pathology and Experimental Therapy
Faculty of Medicine and Health Sciences – University of Barcelona
08907 L'Hospitalet de Llobregat
Barcelona, Spain
E-mail: allobet@ub.edu
Phone: +34-934024279
ORCID: 0000-0001-5797-6782

Odorants stimulate olfactory sensory neurons (OSNs) to create a bilateral sensory map defined by a set of glomeruli present in the left and right olfactory bulbs. Using *Xenopus tropicalis* tadpoles we challenged the notion that glomerular activation is exclusively determined ipsilaterally. Glomerular responses evoked by unilateral stimulation were potentiated following transection of the contralateral olfactory nerve. The gain of function was observed as early as 2 hours after injury and faded away with a time constant of 4 days. Potentiation was mediated by the presence of larger and faster calcium transients driving glutamate release from OSN axon terminals. The cause was the reduction of the tonic presynaptic inhibition exerted by dopamine D_2 receptors. Inflammatory mediators generated by injury were not involved. These findings reveal the presence of a bilateral modulation of glomerular output driven by dopamine that compensates for imbalances in the number of operative OSNs present in the two olfactory epithelia. Considering that the constant turnover of OSNs is an evolutionary conserved feature of the olfactory system and determines the innervation of glomeruli, the compensatory mechanism here described may represent a general property of the vertebrate olfactory system to establish an odor map.

INTRODUCTION

Olfactory glomeruli are spherical regions of neuropil that contain the first synapse for processing olfactory information and form the glomerular layer of the olfactory bulb. Despite variations in number or size among vertebrate species, glomeruli show an evolutionarily conserved synaptic connectivity (Shepherd, Chen, and Greer 2004). Glomerular input comes from axon terminals of olfactory sensory neurons (OSNs) expressing the same odorant receptor that transfer information to the dendrites of mitral cells. Synaptic transmission between OSNs and mitral cells is regulated by inhibitory and excitatory contacts established with juxtaglomerular neurons. This connectivity allows that upon exposure to odorants only a defined set of glomeruli is activated, creating an odor map (Mombaerts et al. 1996). Glomeruli exhibit an anatomical and functional symmetrical distribution in the left and right olfactory bulbs, therefore, the sensory map created in the olfactory bulb is bilateral and is generated by homologous glomeruli reflecting the contribution of the two nasal cavities (Lodovichi 2021; Belluscio and Katz 2001).

OSNs originate in the olfactory epithelium and are subject to a continuous turnover throughout life (Holl 2018). An efficient neuronal replacement is accomplished by the rapid connection of newborn OSNs to the olfactory bulb. For example, in *X. tropicalis* tadpoles OSNs can establish functional synapses in a time window of 4 days (Terni et al. 2017) and, in mice, it takes a week for newborn OSNs to get inserted in the olfactory bulb through a *plug-and-play* mechanism (Browne, Crespo, and Grubb 2022). The balance existing between the elimination of OSNs and their insertion in olfactory bulb circuitry likely determines a range of input neurons innervating a glomerulus, rather than a constant, precise figure. In this context, how the formation of an odor map accounts for possible variations in the number of input neurons is unknown. Considering that OSNs exclusively form ipsilateral synapses (Shepherd, Chen, and Greer 2004) and release glutamate with near-maximal release probability (Murphy

et al. 2004), the possible crosstalk balancing the individual contribution of bilaterally distributed glomeruli remains unknown, because their high output gain is assumed to be defined unilaterally.

Here, we take advantage of the experimental capacities offered by *Xenopus tropicalis* tadpoles to assess whether the output of a genetically labelled glomerulus (Terni et al. 2017; Terni and Llobet 2021), is solely determined by ipsilateral stimulation. In vivo recordings carried out after disrupting the contribution of the contralateral pathway, challenged this notion. Our results show that the tonic inhibition of glomerular responses exerted by dopamine D_2 receptors is bilaterally shaped to compensate for differences in the number of OSNs innervating the contralateral olfactory bulb. Considering the evolutionary conserved developmental, morphological, and functional features of the *Xenopus* tadpole olfactory system (Menini 2010; Manzini, Schild, and Di Natale 2022), the homeostatic mechanism here described might represent a general rule to the formation of an integrated odor map in vertebrates.

MATERIALS AND METHODS

Animals

Ethical procedures were approved by the regional government (Generalitat de Catalunya, experimental procedure #10753). *Xenopus tropicalis* were housed and raised according to the standard protocols of the animal facilities of the University of Barcelona. Tadpoles were obtained by natural mating and kept in tanks at 25 ºC. *Xenopus* water conductivity was adjusted to 700 $\mu s \cdot cm^{-1}$, pH=7.5. Tadpoles at stage 47-52 of the Nieuwkoop–Faber criteria (Nieuwkoop and Faber 1956) were used for the experiments. The *X. tropicalis* transgenic line *Dre.mxn1:GFP* (RRID:NXR_1111) was used for the visualization of a discrete population of OSNs (Terni et al. 2017; Terni and Llobet 2021) and for carrying out electrophysiological recordings in a genetically defined glomerulus. Labelling of OSNs was

53 consistent in all animals of this transgenic line. Calcium imaging was performed in the *X.*
54 *tropicalis* transgenic line *ElasGFP:Tubb2b-GCaMP6s* (RRID:NXR_1123). In vivo detection
55 of reactive oxygen species (ROS) was carried out in tadpoles of the *X.laevis* transgenic line
56 *Hsa.UBC-Gal4;UAS:HyPer-YFP* (RRID: NXR_0127).

57 To apply surgical procedures, *Xenopus* tadpoles were anesthetized in 0.02% MS-222
58 and transferred to a wet nitrocellulose filter paper placed under a stereomicroscope. Iridectomy
59 scissors were used for the unilateral transection of an olfactory nerve or the bilateral transection
60 of optic nerves. Tadpoles were returned to water tanks after surgery.

61

62 **Electrophysiology**

63 *X. tropicalis* tadpoles were anesthetized in 0.02% MS-222 and the portion of skin
64 covering the olfactory bulb was removed. Animals were transferred to a well fabricated in a
65 dish coated with silicone elastomer. A coverslip restricted tadpole movements and left
66 olfactory placodes and bulbs accessible (Terni et al. 2018). The dish was placed on the stage
67 of an upright microscope (Zeiss, Axioexaminer A1, Oberkochen, Germany) and was
68 continuously perfused with *Xenopus* Ringer containing (in mM):100 NaCl, 2 KCl, 1 $CaCl_2$, 2
69 $MgCl_2$, 10 glucose, 10 HEPES, 240 mOsm/kg, pH=7.8, supplemented with 1 μM d-
70 tubocurarine to prevent muscle contractions. All salts and drugs were from Sigma-Aldrich
71 (Sant Louis, MO). CGP-36742 was from Novartis Pharmaceuticals (Basel, Switzerland). To
72 carry out extracellular recordings a borosilicate pipette filled with *Xenopus* ringer was targeted
73 to the olfactory glomerulus showing GFP fluorescence. Signals were acquired using a
74 Geneclamp 500A amplifier (Molecular Devices, San Jose, CA) and digitized at 10 kHz using
75 a National Instruments NI-USB-6341 DAC board (National Instruments, Austin, TX)
76 controlled by mafPC software (courtesy of M. A. Xu-Friedman, University at Buffalo, NY).

77 The recorded changes of the LFP were low pass filtered below 100 Hz and analyzed with Igor
78 Pro 9.0 (Wavemetrics, OR).
79 Methionine was chosen as odor stimulus based on its broad capacity to stimulate OSNs
80 in *Xenopus laevis* tadpoles (Manzini and Schild 2004). A puff of 200 μM methionine solution,
81 obtained by diluting a 10 mM stock solution prepared in *Xenopus* Ringer (pH=7.8), was applied
82 on the ipsilateral olfactory epithelium to the recorded glomerulus. The amino acid was
83 delivered through a 0.25 mm diameter fused silica capillary (World Precision Instruments,
84 Hertfordshire, UK) positioned on the top of a nasal cavity. The timing of application was
85 controlled via a TTL pulse. The characteristic odor evoked glomerular response was obtained
86 by averaging LFP changes triggered by sequential stimulations applied at 2 min intervals. The
87 local application of antagonists was carried out by transiently applying 20 psi pressure to the
88 pipette holder inlet. Approximately 1 μL of the pipette solution was delivered to the
89 glomerulus.
90
91 **Imaging**
92 Quantification of OSNs present in the olfactory epithelium of *Dre.mxn1:GFP* tadpoles
93 was performed in an inverted LSM880 confocal microscope (Zeiss) using animals anesthetized
94 in 0.02% MS-222. The number of neurons was estimated from maximal intensity projections
95 in confocal Z-stacks. To selectively eliminate GFP positive OSNs the 2Phatal method (Hill et
96 al. 2017) was adapted to confocal microscopy. Tadpoles were immersed for 15 minutes in
97 *Xenopus* water containing 5 μg/mL Hoechst 33342 and anesthetized in 0.02% MS-222.
98 Animals were placed dorsally on a 25 mm glass #1.5 coverslip acting as the bottom of an
99 imaging chamber and transferred to the microscope stage. The right olfactory epithelium,
100 located contralaterally to the recording site, was imaged with a 10X Plan Apo objective,
101 NA=0.45 (Zeiss). The digital zoom was set to 3.5. Photobleaching was carried out using

102 ZenBlue software (Zeiss) in 4 to 6 regions of interest (ROIs) containing two or more GFP
103 positive OSNs. Animals were next returned to water tanks.

104 The *X. tropicalis* transgenic line *ElasGFP:Tubb2b-GCaMP6s*, where the neuronal β-
105 tubulin promoter drives the expression of the calcium sensor GCaMP6s, was used to visualize
106 the activation of olfactory glomeruli. As for in vivo electrophysiology, tadpoles were
107 anesthetized in 0.02% MS-222, placed in a recording dish and transferred to the stage of an
108 upright microscope (Zeiss, Axioexaminer A1). Tadpoles were continuously perfused with
109 *Xenopus* Ringer containing 1 μM d-tubocurarine. Imaging was carried out at 76 Hz using a
110 Maico MEMS confocal unit (Hamamatsu Photonics, Hamamatsu City, Japan). A 40X, 0.75
111 NA water immersion W-N-Achroplan objective (Zeiss) was used. Odorant stimulation was
112 performed as described for electrophysiology experiments. The timing of methionine
113 application was synchronized with image acquistion (HCImage software, Hamamatsu
114 Photonics) using a Master 8 stimulator (AMPI, Jerusalem, Israel). In experiments where
115 imaging was coupled to recordings of the LFP, the electrode was targeted to the lateral
116 glomerular cluster. All signals were synchronized using a Master 8 stimulator.

117 Raw fluorescence image sequences were used to construct ΔF/F movies according to
118 the relationship $(F-F_0)/F_0$, where F_0 corresponded to the basal fluorescence levels obtained
119 during 1 s before stimulation. ΔF/F sequences were next subsampled by averaging groups of
120 10 frames to identify putative glomeruli, which were defined as 10-20 μm diameter round
121 structures consistently responding to sequential stimulations applied at 2 min intervals. The
122 selected ROIs were transferred to the original raw fluorescence movie to quantify increases in
123 basal intracellular calcium levels. A ROI showing ΔF/F increases evoked by methionine
124 application to the ipsilateral olfactory epithelium that were ≥3 SDs above baseline levels was
125 considered as a single glomerulus. The temporal response was quantified using Igor Pro 9
126 software (Wavemetrics, OR).

127 The production of ROS in the *X. laevis* HyPer-YFP was evaluated after transection of
128 a single olfactory nerve. Tadpoles were imaged in an inverted confocal LSM 900 microscope
129 (Zeiss) using a Plan-Apochromat 20X, 0.8NA objective. Hyper-YFP was excited at 405 nm
130 and 488 nm. ROS levels were estimated from the relationship obtained between HyPer-YFP
131 excited at 488 nm and 405 nm (Love et al. 2013).
132
133 **Uncaging of Rubi-glutamate**
134 Rubi-glutamate was added to the pipette solution at a final concentration of 300 μM.
135 Procedures were carried out considering the high sensibility to light of the caged compound
136 (Fino et al. 2009). To prevent spontaneous activation of Rubi-glutamate, glass pipettes were
137 coated with beeswax. The electrode was positioned above the lateral region of the glomerular
138 layer using dim transmitted light. Next, the GFP labelled glomerulus was targeted using blue
139 light attenuated with a ND filter (0.5 OD). Approximately 1 μL of the pipette solution was
140 injected in the glomerulus. Upon certifying that the recording of LFP signal was stable for 2
141 min, a TTL signal opened a shutter (Lambda SC, Sutter Instrument, Novato, CA) for 500 ms
142 to deliver blue light (470±20 nm) through the epifluorescence port. A diaphragm restricted
143 light application to the region targeted by the electrode.
144
145 **Statistical analysis**
146 For statistical analysis, paired and unpaired t-test were used to evaluate differences
147 between two experimental groups. Comparisons among three or more groups were performed
148 using one way ANOVA followed by multiple comparison Tukey's HSD test. Average values
149 are expressed as mean±s.e.m. Statistical analysis was carried out using Igor Pro software.
150
151

152 **RESULTS**

153

154 **Characterization of odor evoked responses in a genetically defined glomerulus**

155 The *Xenopus tropicalis* line *Dre.mxn1:GFP* allows the identification of an olfactory
156 glomerulus located laterally and innervated by a discrete population of OSNs (Terni et al. 2017;
157 Terni and Llobet 2021). We targeted an electrode to the left GFP labelled glomerulus and
158 recorded changes in the Local Field Potential (LFP) evoked by ipsilateral stimulation with an
159 amino acid acting as a waterborne odorant (Figs. 1A and B). An olfactory response was
160 triggered by 100 ms application of 200 μM methionine to the olfactory epithelium, thus
161 confirming the ability of *Xenopus* tadpoles to detect amino acids (Manzini et al. 2007).
162 Stimulation evoked a negative deflection of the LFP that resembled responses obtained in the
163 glomerular layer of rats upon sniffing odors (Chaigneau et al. 2007). A main difference
164 between negativities recorded in *X. tropicalis* and those found in rodents is that the latter are
165 respiration-locked, while in tadpoles there was a single deflection that recovered with a half
166 time ranging from 1 to 4 s.

167 An estimate of the spatial extent of the LFP signal was obtained by evaluating responses
168 after changing the position of the recording electrode. The characteristic profile of LFP
169 changes disappeared when the pipette was directed to the mitral cell layer (Fig. 1C), thus
170 illustrating they were confined to the glomerular layer. The consistent success rate (85%,
171 n=269) obtained by targeting the GFP labelled glomerulus with the recording electrode
172 decreased to 50% (n=36) when random locations linearly spaced by 50 μm were tested within
173 the glomerular layer. The example shown in Fig. 1D illustrates how the characteristic response
174 to methionine was obtained only in one out of four positions tested. These observations could
175 be explained by the capacity of the electrode to detect only activated glomeruli (Manzini et al.
176 2007). The high success rate of the recordings guided by fluorescence support that the GFP

177 labeled glomerulus responded to methionine. Considering many olfactory glomeruli in
178 *Xenopus* tadpoles are broadly tuned (Manzini et al. 2007), it is conceivable that the recorded
179 glomerulus was also activated by other waterborne odorants, which were not tested in the
180 current study.

181 The LFP signal likely sampled the entire volume of 15765±2119 μm^3 (n=33) defined
182 by fluorescence but, as the lateral cluster of glomeruli is markedly involved in the detection of
183 amino acids (Weiss, Manzini, and Hassenklöver 2021), the influence of adjacent glomeruli
184 cannot be ruled out from the start. Considering the labelled glomerulus had a diameter of ~30
185 μm (Fig. 1E) and there was a 50 μm axial resolution to obtain independent readouts (Fig. 1D),
186 only a portion of surrounding glomeruli could theoretically participate in the observed LFP
187 signal. The glomerular layer of the amphibian olfactory bulb is loosely organized compared to
188 mammals, as glomerular units show different sizes and lack ensheathing astrocytes (Nezlin and
189 Schild 2000; Gaudin and Gascuel 2005). The absence of a homogeneous distribution of
190 glomeruli, added to the dorsorostral location of GFP labelled axon terminals (Fig. 1E),
191 restricted the number of adjacent glomeruli that could theoretically contribute to the recorded
192 LFP signal to those found ventrally or caudally. Even if 50% of such units were activated by
193 methionine, the decay of the LFP following a relationship inversely related to distance to the
194 recording site, as reported for the mammalian olfactory bulb (Karnup et al. 2006), would
195 minimize their contribution. Altogether indicates that methionine application to the olfactory
196 epithelium reliably activated the lateral glomerulus labeled by GFP in the *Dre.mxn1:GFP* line.

197 Glomerular responses were assayed by repetitive stimulation at two-minute intervals
198 and all negativities showed a comparable profile (Fig. 1B). The peak of the negative deflection
199 was reached ~1 s after olfactory stimulation. The characteristic LFP response of any given
200 tadpole was obtained by averaging 5 to 8 consecutive stimulations. Local application of 100
201 μM CNQX decreased LFP negativities by approximately 50% (Fig. 2A). The reduction was

202 comparable when 100 μM D-AP5 was used instead of CNQX (Fig. 2B). The concomitant
203 application of both drugs produced an additive effect that reduced responses by 70% (Fig. 2C
204 p=0.0004, paired t-test), thus evidencing their synaptic origin, as well as the involvement of
205 AMPA and NMDA receptors. These results are comparable to those obtained in rats
206 (Chaigneau et al. 2007; Lecoq, Tiret, and Charpak 2009), which validates our experimental
207 configuration to record LFP responses in a region defined by a genetically labelled glomerulus.
208 The onset phase of negativities was particularly sensitive to CNQX and AP5,
209 suggesting that it was reflecting the involvement of receptors activated by glutamate release
210 from OSN axon terminals. A way to test this possibility was to induce a jump in glutamate
211 concentration inside the glomerulus and assay whether a change in the LFP signal occurred.
212 We targeted the electrode to the lateral GFP glomerulus, injected *Xenopus* ringer solution
213 containing 300 μM Rubi-glutamate and uncaged it using a flash of blue light (Fino et al. 2009).
214 A transient negativity was induced by a 500 ms pulse of light, which was reproduced by
215 repeated stimulations (Fig. 2D). The average amplitude of LFP_{peaks} was of 30±3 μV (n=21, 3
216 tadpoles). This observation supported that the initial phase of LFP negativities was caused by
217 the marked increase in the extracellular concentration of glutamate secreted by OSN axon
218 terminals converging in a glomerulus.
219 The contribution of inhibitory neurotransmission mediated by $GABA_A$ receptors was
220 negligible because no variations in LFP changes evoked by methionine were observed after
221 local application of 1 mM picrotoxin (Fig. 2E). To certify that ipsilateral stimulation of OSNs
222 was the trigger of recorded responses, we investigated the effect of methionine application to
223 the contralateral epithelium. Negativities disappeared (Fig. 2F), thus demonstrating that
224 glomerular activation was exclusively unilateral. In 37% of the tadpoles studied (n=174) the
225 negativity was preceded by a transient positivity (Fig. 1B). When present, this LFP deflection
226 was not modified by glutamate and $GABA_A$ receptor antagonists (Figs. 2A and E), thus

227 indicating it was unrelated to synaptic mechanisms. As the positivity was caused by the
228 application of olfactory stimuli and always occurred before the synaptic response, it is possible
229 to consider its origin in cellular structures conveying peripheral information to the olfactory
230 bulb such as the layer of nerve fibers.
231
232 **Odor evoked responses depend on the number of input neurons.**
233 The amplitude of LFP negativities decreases during the reinnervation of the glomerular
234 layer after olfactory nerve transection (Terni et al. 2017), which suggests that LFP changes are
235 related to the number of OSNs axons projecting to glomeruli. If odor evoked responses were
236 indeed related to glomerular input, the smallest negativities should take place in the earliest
237 developmental stages. This possibility was confirmed by observing that GFP positive neurons
238 found in the olfactory epithelium increased with development and their number followed an
239 empirical linear relationship related to olfactory nerve width for tadpoles found between NF
240 stages 47 and 54 (Fig. 3A, r^2=0.96). The peak of the LFP response was also related to olfactory
241 nerve width but followed an exponential fit. Negativities reached a steady-state value (Fig.
242 3A), thus suggesting the achievement of a consolidated glomerular activation in this
243 developmental time interval. The presence of constant glomerular responses for NF stages >50
244 coincides with the consolidation of the basic structure of the olfactory bulb, which remains
245 constant through larval life (Byrd and Burd 1991). LFP changes were empirically described
246 by the function $LFP_{peak}=LFP_{steady\text{-}state}+Ae^{-r\cdot ONW}$ that associated the maximum change in the LFP
247 (in μV) to olfactory nerve width (ONW, expressed in μm). The fit revealed an increase rate (r)
248 of 0.13 μm^{-1} starting at a diameter of 21 μm, which corresponds to the thinnest olfactory nerves
249 present during development around NF stage 40. Considering the linear correlation found
250 between the number of GFP positive OSNs and the width of olfactory nerves, it was possible
251 to rewrite the exponential fit as a function of the number of OSNs. The estimated peak

252 negativity in the LFP could thus be obtained according to $LFP_{peak}=108-1866\cdot e^{-0.11*\cdot OSNs}$ for a
253 given number of OSNs in the olfactory epithelium. On average, an olfactory epithelium
254 contained 30±2 GFP positive OSNs, ranging from 24 to 39 labelled neurons (n=44) and, this
255 relationship provided a quantitative association of the amplitude of odor evoked responses to
256 the insertion of OSNs in a glomerulus during normal development.
257
258 **Odor evoked responses are potentiated by the injury of the contralateral olfactory**
259 **pathway.**
260 Transection of both olfactory nerves causes a silencing of the capacity of *X. tropicalis*
261 tadpoles to perceive odors (Terni et al. 2017). Since animals having a single nerve still display
262 normal olfactory guided behavior, we investigated how information is transmitted in the
263 absence of the mirror pathway. Olfactory nerve transection caused a potentiation of evoked
264 LFP negativities in the recorded contralateral olfactory glomerulus (Fig. 3B) that was already
265 observed two hours after injury (Fig. C). All tadpoles investigated showed odor evoked
266 responses above the expected LFP_{peak} level for the range of developmental stages analyzed.
267 By reaching a maximum potentiation between 24 and 48 hours after transection, LFP_{peak}
268 responses returned to control values following an exponentially recovery phase that took place
269 with a time constant of 100 hours (Fig. 3D). The overall duration of potentiation coincided
270 with the approximately two weeks required to reform the glomerular layer upon olfactory nerve
271 transection (Terni et al. 2017), suggesting that the increase of glomerular output occurred while
272 the circuitry of the contralateral olfactory bulb was being remodeled after injury.
273 LFP_{peak} responses had a strong synaptic contribution because they were dependent on
274 the number of OSNs innervating the glomerulus (Fig. 3A), were sensitive to the application of
275 glutamate receptor blockers (Figs. 2A-C) and could be triggered by glutamate uncaging (Fig.
276 2D). These results complement those obtained in rats showing a correlation of the amplitude

277 of LFP negativities to calcium influx in OSN terminals (Lecoq, Tiret, and Charpak 2009) and
278 EPSPs recorded in mitral cells (Chaigneau et al. 2007). We thus hypothesized that the observed
279 potentiation affected to glutamatergic synapses mediating glomerular activation.
280

281 **Tissue repair mechanisms are not involved in the potentiation of odor evoked responses**

282 Since inflammatory mediators affect to synaptic functions (Wu et al. 2015), we
283 evaluated the involvement of molecules released by injury using two different strategies. First,
284 to observe if sensory nerve damage were enhancing LFP_{peak} responses, we sectioned both optic
285 nerves (Fig. 4A). Even though optic and olfactory nerves show substantial functional and
286 anatomical differences, the nature of the injury, as well as the distance to the recorded site was
287 comparable between optic and olfactory nerve transection. On these bases we assumed that
288 the effect generated by diffusible inflammatory mediators, or the capacity to mobilize cells
289 mediating inflammation, should be comparable in both experimental conditions. LFP
290 negativities recorded 24h to 48h after bilateral optic nerve transection showed an amplitude of
291 86±6 μV (n=17). This value was expected by normal development but was significantly lower
292 ($p=1.92\cdot10^{-5}$, unpaired t-test), than the amplitude of 186±16 μV (n=14) found in tadpoles
293 subjected to transection of the contralateral olfactory nerve (Fig. 4B).

294 Secondly, we investigated the release of reactive oxygen species (ROS), which are key
295 to trigger tissue repair mechanisms in tadpoles (Love et al. 2013). The *Xenopus laevis* line
296 HyPer-YFP displays a ubiquitous expression of the H_2O_2 sensor HyPerYFP that allows the in
297 vivo detection of ROS created by wounds (Love et al. 2013; Niethammer et al. 2009). Two
298 hours after unilateral olfactory nerve transection there was an increase in H_2O_2 levels that was
299 restricted to the cells present at the injury site (Fig. 4C). ROS levels remained unaltered in the
300 olfactory epithelium and in both olfactory bulbs. Moreover, the amplitude of odor evoked
301 changes in the LFP were unaffected by the presence 200 μM apocynin or 2 μM

302 diphenyleneiodonium, two blockers of ROS production (Fig. 4D, p=0.36, ANOVA followed
303 by Tukey's test) that block tail regeneration at these concentrations (Love et al. 2013). All
304 these findings together suggested that the enhancement of glomerular responses was unlikely
305 caused by inflammatory mediators or the activation of fundamental tissue repair mechanisms
306 operating in tadpoles and, revealed the presence of an intrinsic compensatory mechanism
307 operating in the olfactory system.
308

309 **Potentiation of odor evoked responses is of presynaptic origin**

310 The activation of individual glomeruli was imaged in the transgenic *X. tropicalis* line
311 *tubb2b:GCaMP6s* to gain insight on a putative synaptic mechanism acting on the bilateral
312 balance of odor evoked responses. Ipsilateral application of 200 μM methionine to the
313 olfactory epithelium activated a defined set of glomeruli, which were identified as round, 10-
314 20 μm diameter structures. Same glomeruli reacted to three or more consecutive methionine
315 stimulations (Fig. 5A). Responses detected as calcium transients showed comparable
316 amplitudes and temporal profiles (Fig. 5B), suggesting that the simultaneous activation of
317 sparse glomeruli contributed to the elaboration of an olfactory map. Two lines of evidence
318 support that calcium increases originated in presynaptic terminals of OSNs. First, because the
319 *tubb2b* promoter primarily targets OSNs over olfactory bulb interneurons. A detailed
320 characterization carried out in *X. laevis* tadpoles shows that *tubb2b* efficiently drives expression
321 of a genetically encoded fluorescent reporter in OSNs but fails to label periglomerular neurons
322 positive for calretinin or tyrosine hydroxylase and only targets 24% of mitral cells (Daume et
323 al. 2022). The convergence of multiple fluorescent OSN axon terminals on a single glomerulus
324 and a minimal presence of labelled juxtaglomerular and mitral cells, makes *X. tropicalis*
325 *tubb2b:GCaMP6s* tadpoles well-suited to detect the presynaptic component of glomerular
326 responses. Second, because the simultaneous imaging of glomerular activation and recording

327 of LFP negativities revealed a temporal correlation of the two signals (Fig. 5C). This
328 observation matches the findings of a previous study carried out in rats, where a comparable
329 relationship was described between responses detected in OSN axon terminals labelled with a
330 high affinity calcium dye and LFP signals (Lecoq, Tiret, and Charpak 2009). Although tadpoles
331 of the *tubb2b-GCaMP6s* line consistently showed glomeruli activated by methionine, the
332 coupling of imaging to LFP signals had a low success rate. Even though the electrode was
333 targeted to the lateral glomerular cluster, which is the region expected to concentrate responses
334 to amino acids (Weiss, Manzini, and Hassenklöver 2021), LFP negativities were detected in
335 only 33% of animals tested (n=17/52). This figure is below the 50% found after the
336 performance of recordings in random locations of the glomerular layer (Fig. 1D) but it is higher
337 than the ~25% success rate found in *X. laevis* tadpoles (Manzini et al. 2007). This observation
338 reinforces the selectivity of LFP recordings to detect the output of a single glomerulus, which
339 in this set of experiments was coupled to the fluorescent response found in closest apposition
340 to the tip of the pipette. Altogether indicates that the readouts of glomerular input and output
341 were reported by transient increases in GCaMP6s fluorescence and LFP signals, respectively.

342 A hallmark of contralateral olfactory nerve transection was the development of faster
343 LFP negativities. The time constant to reach the LFP_{peak} shortened significantly (p=0.017,
344 unpaired t-test) from 1.05±0.1 s (n=46 tadpoles) to 0.71±0.1 s (n=39 tadpoles), whilst the
345 recovery phase was unaffected (Fig. 5D, p=0.79, unpaired t-test). The faster glomerular output
346 likely had a presynaptic origin, because calcium transients were larger and showed faster onset
347 kinetics after contralateral nerve transection (Figs. 5E and F). The average amplitude increased
348 more than two-fold (p=0.02, unpaired t-test) and the time constant describing the rise time
349 shortened significantly (p=0.0003, unpaired t-test) in tadpoles with a transected olfactory nerve
350 compared to control animals (Fig. 5F). The slow kinetics of GCaMP6s prevented a precise
351 temporal association between calcium buildup and the onset of LFP changes (Fig. 5C) and a

352 certain saturation of the high affinity calcium indicator in axon terminals was also expected.
353 But, despite these limitations to quantitative analysis, the changes reported by GCaMP6s
354 showed an overall enhancement of cytosolic calcium levels mediating neurotransmitter release.
355 We next sought to investigate which regulatory mechanisms acting on OSN axon terminals
356 were controlled bilaterally to alter glomerular output.
357

358 **Dopamine D_2 receptors modulated by contralateral glomerular input mediate**
359 **presynaptic inhibition**

360 Presynaptic inhibition regulates neurotransmission in olfactory glomeruli (McGann
361 2013). Discrete populations of juxtaglomerular neurons that release GABA or dopamine
362 activate $GABA_B$ or D_2 receptors present in presynaptic terminals of OSNs to lower glutamate
363 release (Wachowiak et al. 2005; Wachowiak and Cohen 1999). Evidence points out that this is
364 a tonically active mechanism (Pírez and Wachowiak 2008), thus meaning the normal
365 processing of odor information relies on a certain level of inhibition of glomerular output. To
366 evaluate the possible involvement of dopamine or GABA in the potentiation of LFP_{peaks}
367 observed after contralateral olfactory nerve transection, we locally applied antagonists of D_2
368 and $GABA_B$ receptors to the recorded glomerulus. Odor evoked responses were enhanced by
369 raclopride, a D_2 antagonist, in tadpoles with their olfactory pathways intact (Fig. 6A). The
370 average negativity of 73±5 μV (n=8) experimented a gradual increase in the presence of 300
371 nM raclopride that reached 128±16 μV, 20 min after its application (Fig. 6B, p=0.012, paired
372 t-test). The potentiation of odor evoked responses caused by the D_2 antagonist was not
373 observed in tadpoles with the contralateral olfactory nerve transected. Baseline negativities of
374 133±24 μV (n=11) were minimally increased by raclopride, changing to 156±33 μV (n=11,
375 p=0.16, paired t-test), 20 min after drug application.

376 The time course of the increase in LFP_{peaks} observed in control tadpoles was well
377 described by a Hill equation, reporting a time required to reach the 50% of the maximal increase
378 of approximately 20 min (Fig. 6C). The time window describing the effect of raclopride could
379 be attributed to disinhibition, since the primary target of presynaptic D_2 receptor activation is
380 the decrease of cAMP levels and a consequent lowering of neurotransmitter release (Kaneko
381 and Takahashi 2004). The potentiation mediated by raclopride was comparable to the increase
382 in LFP_{peaks} caused by olfactory nerve transection (Fig. 6B, p=0.46, unpaired t-test). These
383 results indicated that the tonic inhibition of glomerular output was comparably reduced either
384 by directly inhibiting D_2 receptors, or, by surgically transecting the contralateral olfactory
385 nerve. Further evidence for the involvement of D_2 receptors was obtained by simultaneously
386 imaging GCaMP6s fluorescence and LFP signals (Fig. 6D). In the illustrated example
387 raclopride shortened the time constant (τ) to reach the calcium peak from 1.3 s to 0.5 s and
388 potentiated LFP changes by 50%, thus reproducing the effect of contralateral olfactory nerve
389 transection on glomerular input and output, respectively (Figs. 3C and 5F). On average
390 raclopride reduced τ from 1.27 s to 0.8 s (n=4 tadpoles, p=0.02, paired t-test), evidencing that
391 the potentiation of glomerular responses was mediated by a faster buildup of presynaptic
392 calcium levels that took place after antagonizing the inhibitory action of D_2 receptors.
393 Finally, we explored whether presynaptic $GABA_B$ receptors activated by
394 juxtaglomerular neurons (McGann 2013) could mediate a synergic effect to D_2 receptors. This
395 possibility was investigated by applying the selective $GABA_B$ antagonist CGP-36742. LFP_{peaks}
396 remained unchanged (Figs. 6E and F, p=0.77, paired t-test). A significant tonic inhibition by
397 GABA was thus ruled out, revealing dopamine was the main neurotransmitter inhibiting
398 glomerular output in the glomerular layer of *Xenopus* tadpoles.
399

400 **Effect on glomerular responses of the partial elimination of mirror olfactory sensory**
401 **neurons.**

402 To shed light on the synaptic connectivity involved in the contralaterally driven
403 potentiation of glomerular output we modified the 2Phatal technique (Hill et al. 2017) to
404 eliminate groups of GFP positive OSNs using a conventional confocal microscope (Fig. 7A).
405 Tadpoles were placed during 15 minutes in *Xenopus* water containing 5 μg/mL Hoechst 33342,
406 which is a membrane permeable dye with affinity for nucleic acids, to label all cells found
407 within the olfactory epithelium. Damage was exerted by photobleaching groups of cells found
408 in regions of interest (ROIs) that contained two or more GFP positive OSNs. Efficient
409 photobleaching of the nuclear label caused cell death, which was certified by the observation
410 of condensed nuclei after 24 hours (Fig. 7A). The use of the confocal microscope precluded
411 the achievement of single cell ablation but supported the robust elimination of cells within
412 ROIs. Olfactory epithelial cells found outside the selected areas remained unaffected.
413 Photobleaching was typically carried out in 4 to 6 ROIs, thus resulting in the elimination of 10
414 to 15 OSNs. Considering an epithelium contained on average ~30 GFP positive OSNs, the
415 protocol led to an estimated 30 to 50% reduction of OSNs innervating the right GFP labeled
416 glomerulus. Since the viability of tadpoles subjected to a more extensive reduction of
417 fluorescent OSNs was compromised, all animals investigated still had a significant number of
418 functional GFP labelled OSNs after photoablation.

419 A characteristic of the recorded odor evoked glomerular responses was their
420 reproducibility. For a given tadpole, LFP negativities occurred after successive stimulations
421 with a comparable profile (Figs. 1B, 2A, 4A), and showed an average variance in their
422 amplitude of 386±96 μV^2 (n=17). Variance of the responses obtained increased more than
423 three-fold in tadpoles subjected to transection of the olfactory nerve (see for example Fig. 3B),
424 reaching an average value of 1488±280 μV^2 (n=14). An enhancement of variance was thus

425 associated to the potentiation observed in response to olfactory nerve transection. Incubation
426 of tadpoles with Hoechst 33342 neither modified the amplitude nor the variance of LFP_{peaks}
427 (Fig. 7B). LFP negativities in tadpoles presenting a decimated population of contralateral GFP
428 positive OSNs showed an increase in LFP_{peaks} from 80±5 μV (n=17) to 89±7 μV (n=10, p=0.32,
429 unpaired t-test) and in variance to 1024±475 μV^2 (n=10, p=0.21, unpaired t-test).

430 The non-significant changes in LFP_{peaks} amplitude and variance induced by selective
431 photoablation could be attributed to the limited suppression of GFP labeled OSNs and it was
432 not possible to establish through this experimental approach the effect of the complete
433 suppression of cognate neurons. LFP_{peaks} variance and amplitude were linearly related (r=0.65)
434 considering control and unilaterally transected tadpoles together (Fig. 7C) and in this context,
435 the reduction between 1/3 and 1/2 of the mirror contralateral glomerular input induced a right-
436 shift compared to control values. Considering that the photoablation procedure left most of
437 OSNs present in the olfactory epithelium intact, the observed displacement suggests that
438 topographical relationships established bilaterally could be relevant to establish a
439 contralaterally driven potentiation. Moreover, our results support that bilateral modulation of
440 glomerular output occurs within a graded scale that is inversely related to the contralateral
441 innervation by OSNs.

442

443 **DISCUSSION**

444 Odor evoked responses were recorded as changes of the LFP in an olfactory glomerulus
445 labelled in the *Dre.mxn1:GFP X. tropicalis* line (Fig. 1) and showed the following
446 characteristics: *i)* were mediated by glutamatergic synapses (Figs. 2A-C), *ii)* were triggered by
447 ipsilateral stimulation of OSNs (Fig. 2F), and, *iii)* showed an amplitude related to the number
448 of input OSNs (Fig. 3A). These characteristics are comparable to responses recorded in the
449 glomerular layer of living rats where negativities are supported by the activation of glutamate

450 receptors and locked to the respiration frequency (Lecoq, Tiret, and Charpak 2009).
451 Glomerular responses were potentiated by the complete silencing of OSNs projecting to the
452 contralateral olfactory bulb, thus showing the processing of information in the olfactory
453 glomeruli of *Xenopus* tadpoles is not exclusively unilateral and is shaped contralaterally. The
454 observed potentiation was not related to inflammatory mediators associated to injury, because
455 it was caused by a release of the inhibition made by D_2 dopamine receptors present in OSN
456 axon terminals.

457 The similarities between the recordings obtained (Fig. 1B) and those described in rats
458 (Chaigneau et al. 2007), indicate the presence of evolutionary conserved morphological and
459 functional features between both species and therefore, the applicability to vertebrates of the
460 findings here described. Our results achieved using glutamate blockers and uncaging of Rubi-
461 glutamate show that the onset of LFP changes detected in glomeruli is determined by glutamate
462 release from OSNs. The ionic bases supporting the recovery phase of negativities are uncertain
463 but, considering responses obtained by glutamate uncaging were locked to the period defined
464 by the light pulse, the participation of sustained neurotransmitter release is conceivable. This
465 view is also supported by imaging of OMP-synaptopHluorin mice, where continuous synaptic
466 vesicle exocytosis occurs over several seconds in OSN axon terminals (Petzold et al. 2008).

467 The mammalian and amphibian olfactory bulbs display comparable anatomical and
468 cellular organization (Manzini, Schild, and Di Natale 2022) but, it is yet unknown whether the
469 three classes of juxtaglomerular neurons present in rodents: periglomerular, short-axon and
470 external tufted, also exist in *Xenopus*. In mice, short-axon cells are the main source of
471 dopamine to olfactory glomeruli (Kiyokage et al. 2010), however, there is a lack of evidence
472 for such a discrete population in the olfactory bulb of *Xenopus* tadpoles. Dopaminergic neurons
473 are distributed around olfactory glomeruli after NF stage 49 (González et al. 1994) and in adult
474 *Xenopus*, type-I tyrosine hydroxylase positive cells extensively innervate the glomerular layer

475 (Boyd and Delaney 2002). These morphological observations indicate that dopaminergic
476 neurons exist in the glomerular layer of amphibia, but their specific functional properties are
477 unknown. As we did not find evidence for the $GABA_B$ mediated inhibition described in rats
478 (Wachowiak et al. 2005), our results support that dopamine is the main inhibitory
479 neurotransmitter in the glomerular layer of *Xenopus* tadpoles.

480 To understand how tonic dopamine release in the glomerular layer of *Xenopus* tadpoles
481 is affected by the number of contralateral OSNs, it is necessary to have a comprehensive
482 understanding of olfactory bulb connectivity in *X. tropicalis* tadpoles which is currently
483 lacking. Interneurons of the amphibian olfactory bulb might not display the degree of
484 specialization found in rats or mice, however, there is evidence suggesting that type-1 tyrosine
485 hydroxylase positive interneurons are morphologically similar to external tufted cells present
486 in rodents (Boyd and Delaney 2002). External tufted cells show rhythmic activity (Hayar et al.
487 2004), are responsible for constructing a map of homologous glomeruli through intrabulbar
488 connections (Lodovichi, Belluscio, and Katz 2003) and act as gatekeepers of glomerular output
489 (Banerjee et al. 2015). Therefore, if the dopaminergic neurons present in the glomerular layer
490 of *Xenopus* tadpoles play analogous roles to external tufted cells, our results call for
491 considering this group of interneurons as candidates to exert the contralateral regulation of
492 glomerular output.

493 Here, we show that the formation of an odor map in *Xenopus* tadpoles relies on a
494 balanced contribution of the glomerular responses occurring in both olfactory bulbs. Tonic
495 activation of presynaptic D_2 receptors, likely mediated by dopaminergic juxtaglomerular
496 neurons, drives to a constant inhibition of glomerular output. Dopamine release is affected by
497 the number of operative contralateral OSNs so that, in the extreme situation where all mirror
498 olfactory pathways are silenced, dopamine secretion decreases and most of the inhibition is
499 released (Fig. 7D). The consequence is an immediate increase of glomerular responses in the

non-damaged pathway, which results in a compensated output signal. A possible direct contralateral targeting by OSNs, as described for the γ-glomerulus present in *X. laevis* tadpoles (Kludt et al. 2015), was ruled because the population labelled in the *Dre.mxn1:GFP* showed exclusively a unilateral distribution. Interhemispheric connections targeting dopaminergic juxtaglomerular neurons could be established by axons of mitral cells as reported in zebrafish (Kermen et al. 2020). However, the participation of neurons of the lateral pallium cannot be disregarded as it is a main center for olfactory processing (Moreno et al. 2008). Either one of these projecting neurons could be targeting contralateral dopaminergic neurons found in the glomerular layer of *X. tropicalis* tadpoles (Fig. 7D). Although the existence of an intraglomerular circuit controlling dopamine release cannot be disregarded (Banerjee et al. 2015), and, considering the differences existing between olfactory bulb interneurons present in amphibia and mammals (Imamura, Ito, and LaFever 2020), we modeled the simplest scenario based in only one cell type of juxtaglomerular neuron.

The in vivo evidence presented shows that presynaptic D_2 receptors tonically exert an inhibitory action on calcium buildup in OSN axon terminals. This finding is well aligned with previous observations obtained in mouse brain slices (Ennis et al. 2001) and describes a relevant biological scenario for the role of dopamine inhibition in the glomerular layer of the olfactory bulb. Both the suppression of contralateral OSN inputs and the local injection of the D_2 antagonist raclopride enhanced glomerular output, a finding that can be explained by the tight coupling existing between calcium influx and neurotransmitter release in OSN axon terminals (Wachowiak et al. 2005). The likely target of dopamine are N-type voltage gated calcium channels because they are present in presynaptic terminals in olfactory glomeruli (Weiss et al. 2014) and they can be inhibited through multiple mechanisms activated by D_2 receptors (Kisilevsky and Zamponi 2008).

524 Taken altogether our results illustrate a homeostatic mechanism used to compensate a
525 reduced contribution of contralateral OSNs characterized by an enhancement of glomerular
526 output. It is possible that the observed compensation maximizes the role of a pathway relevant
527 to the normal encoding of olfactory information upon transection of an olfactory nerve. Under
528 physiological conditions the contralateral modulation of presynaptic D_2 receptors could be used
529 to correct imbalances in the firing of mitral cells collecting information from bilaterally related
530 glomeruli. Although we can only speculate about such functional role, our lines of evidence
531 show that the mechanism here described is efficiently used for achieving a bilateral
532 compensation of glomerular output in a vertebrate species.
533
534

535 **FIGURE LEGENDS**

536

537 **Figure 1. Recording of odor evoked responses in a genetically defined glomerulus. A)**
538 Schematic diagram illustrating the experimental preparation. A puff of 200 μM methionine was
539 applied during 100 ms to the left olfactory epithelium of *Dre.mxn1:GFP Xenopus tropicalis*
540 tadpoles. Changes in the Local Field Potential (LFP) were measured ipsilaterally with an
541 electrode targeted to the lateral glomerulus formed by axon terminals of olfactory sensory
542 neurons (OSNs) expressing GFP. The inset shows a confocal projection illustrating labelled
543 OSNs (s: soma, a:axon) and the bilateral formation of glomeruli (g). The *Dre.mxn1* promoter
544 also drives GFP expression in the endothelial cells of some blood vessels (e). **B)** Representative
545 glomerular odor evoked response (black) obtained by averaging individual responses (gray) of
546 the LFP following stimulation (arrow). The asterisk shows a positivity that appeared in 37% of
547 the recordings and preceded the characteristic negativity associated to glomerular activation.
548 **C)** Negative deflections of LFP (individual responses, gray; average trace, black) were
549 observed when the recording electrode was placed in the GFP labelled glomerulus but
550 disappeared in the mitral cell layer (MC, red traces). **D)** Experiment showing LFP recordings
551 performed in four different locations of the glomerular layer spaced by 50 μm. The
552 characteristic odor evoked response was observed in only one of the positions tested. The
553 representative glomerular odor evoked response (black) was obtained by averaging individual
554 responses (gray) following stimulation with methionine (arrow). E) Hyperstack projections of
555 the left olfactory bulb of three different *Dre.mxn1:GFP Xenopus tropicalis* tadpoles. The
556 lateral glomerular cluster (L) is always obvious, and some medial projections (M) are evident
557 in two of the illustrated examples. Color scale indicates dorsoventral disposition.

558

559 **Figure 2. Odor evoked responses are mediated by glutamatergic neurotransmission. A)**
560 The representative glomerular odor evoked response (black) was obtained by averaging
561 individual responses (gray) of the Local Field Potential **(**LFP) following stimulation (arrow).
562 In this example, the pipette solution contained 100 µM CNQX and upon local injection of 1
563 µL, there was a reduction in the amplitude of LFP negativities. **B)** Mean LFP changes obtained
564 under control conditions (n=21) were reduced after the application of 100 µM CNQX (n=8),
565 100 µM AP5 (n=5), or both 100 µM CNQX and 100 µM AP5 (n=8). **B)** Box plot illustrating
566 how the initially recorded peak negativities were affected by the application of 100 µM CNQX,
567 or, 100 µM AP5 together with 100 µM CNQX. Boxes represent the median (horizontal line),
568 25th to 75th quartiles, and ranges (whiskers) of the indicated experimental groups. Statistical
569 differences were evaluated using paired t-test. **C**) Rubi-glutamate was injected in the GFP
570 labelled glomerulus and locally uncaged with a 500 ms pulse of blue light (circle). The
571 example shows the change in LFP induced by two flashes (squares) delivered at an interval of
572 9 seconds. **E)** Application of picrotoxin, a $GABA_A$ antagonist, did not modify odor evoked
573 changes. Recordings show average responses (n=9). Statistical differences were evaluated
574 using paired t-test**. F)** Odor evoked LFP changes were exclusively triggered by ipsilateral
575 stimulation. Individual responses are indicated in gray, with the representative average
576 response in black. Contralateral stimuli (yellow) did not modify the LFP, as shown in the
577 average representative response (brown).
578
579
580

581 **Figure 3. Potentiation of odor evoked responses by transection of the contralateral**
582 **olfactory nerve. A)** The number of olfactory sensory neurons (OSNs) and the amplitude of
583 odor evoked negative deflections of the Local Field Potential (LFP) were related to olfactory
584 nerve width according to linear and exponential functions, respectively. Individual data points
585 are represented by circles (n=48). Each bin indicates the mean ± standard error of n=6 tadpoles.
586 The dotted line indicates the steady-state LFP amplitude reached during development. **B)**
587 Representative odor evoked response (red; individual responses, gray) obtained 24 h after
588 contralateral nerve transection. A solution of 200 μM methionine was used as stimulus (arrow).
589 **C)** Odor evoked LFP changes exhibit amplitudes above the expected values (dotted line as in
590 A) after contralateral olfactory nerve transection at the indicated time points. The dots represent
591 the mean ± s.e.m obtained 2 to 7 hours (n=10), 1 to 2 days (n=14), and 10 to 11 days (n=11)
592 post-injury. There was a 75% increase in animals recorded 1 to 2 days after transection of the
593 contralateral olfactory nerve (red arrow) compared to control tadpoles (dotted line). **D)** Dots
594 (mean ± s.e.m.) connected by a line illustrate odor evoked glomerular responses at the indicated
595 times after injury. The superimposed violin plot displays individual data. Most LFP_{peak} values
596 are above the level expected for the developmental period studied (dotted line as in A).
597

598 **Figure 4. The potentiation of odor evoked responses is not mediated by injury derived**
599 **cues. A)** Odor evoked Local Field Potential (LFP) changes were recorded by an electrode
600 targeted to the GFP-positive glomerulus of *Dre.mxn1:GFP* tadpoles one to two days after
601 bilateral transection of optic nerves. **B)** Peak LFP negativities recorded in tadpoles with
602 sectioned optic nerves did not exhibit the characteristic potentiation observed after transection
603 of the contralateral olfactory nerve, as they remained within the range of values observed
604 during normal development (solid line, as in Fig. 3A). Bins indicate mean±s.e.m., circles show
605 individual values. **C)** Imaging of reactive oxygen species (ROS) two hours after transectioning
606 one olfactory nerve (arrow). The ratio between the fluorescence emitted by HyPer-YFP when
607 excited at 488 nm and 405 nm is indicated in pseudocolor. Notice that ROS were increased at
608 the injury site but remained at basal levels in both olfactory bulbs as indicated by the box plot.
609 Each circle shows values collected in a single tadpole. **D)** Block of ROS production by
610 incubating tadpoles with 200 μM apocynin (n=10) or 2 μM diphenyleneiodonium (DPI, n=5)
611 did not modify the amplitude of odor evoked LFP responses recorded 24 h after contralateral
612 olfactory nerve transection (n=10). Boxes represent the median (horizontal line), 25th to 75th
613 quartiles, and ranges (whiskers) of the indicated experimental groups.
614
615

616 **Figure 5. The presynaptic component of glomerular activation is affected by damage to**
617 **contralateral olfactory sensory neurons. A)** Application of a puff of 200 μM methionine to
618 the olfactory epithelium activates a set of glomeruli in the ipsilateral olfactory bulb (arrows) of
619 *tubb2b:GCaMP6*s tadpoles. Images show the relative changes in GCaMP6s fluorescence
620 (ΔF/F) obtained after two sequential stimulations carried out in a single tadpole. **B)** Time
621 course of the responses detected in the glomeruli indicated in A). **C)** Example showing the
622 simultaneous recording of Local Field Potential (LFP) and changes in GCaMP6s fluorescence
623 in the region targeted by the electrode. Colored traces and gray traces show the change in
624 GCaMP6s fluorescence (ΔF/F) and LFP respectively observed after three sequential
625 applications of 200 μM methionine. Black traces show the average ΔF/F and LFP responses.
626 **D)** Kinetics of the change in LFP observed in tadpoles with the contralateral olfactory nerve
627 transected between 2 h and 48h prior to recording. **E)** Intracellular calcium increases detected
628 in glomeruli of control tadpoles with intact olfactory pathways (35 glomeruli, 10 tadpoles,
629 black), and, in tadpoles subjected to the transection of the contralateral olfactory nerve (10
630 glomeruli, 3 tadpoles, red). Each trace indicates the response of a glomerulus to a single
631 stimulus. Solid lines and error bars indicate mean ± s.e.m. **F)** Calcium transients detected in
632 tadpoles with an olfactory nerve transected showed a larger amplitude and a rising phase with
633 a shorter time constant (τ). Boxes in D) and F) represent the median (horizontal line), 25th to
634 75th quartiles, and ranges (whiskers) of the indicated experimental groups. Statistical
635 differences in D) and F) were evaluated using paired and unpaired t-tests, respectively. Circles
636 in D) indicate values obtained for a single tadpole and in F) refer to a single glomerulus.
637
638

639 **Figure 6. Contralateral input modulates presynaptic inhibition mediated by dopamine D_2**
640 **receptors and is involved in the potentiation of glomerular responses. A)** Recordings
641 obtained in a control tadpole showing how the amplitude of Local Field Potential (LFP)
642 responses (gray traces) obtained during a baseline period of 8 minutes increase in a time-
643 dependent manner after local application of 300 nM raclopride, a D_2 receptor antagonist. **B)**
644 Box plot showing the effect of 300 nM raclopride (blue) on the amplitude of LFP responses
645 recorded in tadpoles with full capacity to process odors (control, n=8, black) and tadpoles
646 subjected to the transection of the contralateral olfactory nerve (n=11, red). Boxes represent
647 the median (horizontal line), 25th to 75th quartiles, and ranges (whiskers) of the indicated
648 experimental groups. The effect of raclopride weas evaluated using the paired t-test and the
649 comparison between control and transected groups was performed using the unpaired t-test.
650 **C)** Relative change in LFP responses induced by 300 nM raclopride in control tadpoles and in
651 tadpoles subjected to the transection of the contralateral olfactory nerve. Dots represent mean
652 ± s.e.m. The solid black line illustrates the fit to a Hill equation, defining a T_{50} at 20 minutes.
653 **D)** Simultaneous recording of LFP and changes in GCaMP6s fluorescence in a
654 *tubb2b:GCaMP6s* tadpole. Gray traces and light blue traces show individual responses to
655 sequential stimulations before and after application of 300 nM raclopride, respectively**.**
656 Average responses are shown in black and dark blue. **E)** Application of CGP-36742, a $GABA_B$
657 receptor antagonist, did not modify LFP responses. The box plot compares the amplitude of
658 LFP changes recorded before (gray) and 20 min after local application of 300 μM CGP-36742
659 (green). Statistical differences were evaluated using paired t-test. **E)** Time course of relative
660 LFP changes induced by 300 μM CGP-36742. Dots represent mean ± s.e.m (n=10).
661
662
663

664 **Figure 7. Changes in odor evoked responses caused by selective photoablation of**
665 **olfactory sensory neurons innervating the homologous contralateral glomerulus. A)** Odor
666 evoked Local Field Potential (LFP) changes were recorded one day after the selective
667 elimination of olfactory sensory neurons (OSNs) located in the right nasal cavity. After the
668 identification of GFP-positive OSNs in the epithelium labeled with the nuclear marker Hoechst
669 33342, regions containing ≥2 fluorescent neurons were identified and photobleached. Cell
670 targeting was confirmed by the suppression of the nuclear label. Only cells found within the
671 photobleached areas exhibited fragmented nuclei (arrows) 24 hours after photobleaching. **B)**
672 Examples showing odor evoked responses recorded in a tadpole incubated with Hoechst 33342
673 (black, average), and in a different tadpole 24 hours after the photobleaching of selected regions
674 in the contralateral olfactory epithelium (violet, average). **C)** Plot of variance against the
675 amplitude of LFP_{peaks} in three experimental groups of tadpoles: control (n=17), photoablated
676 (n=10) and subjected to unilateral olfactory nerve transection (n=14). Circles show individual
677 values and dots indicate mean±s.e.m. The line shows a fit through values of control and
678 unilaterally transected tadpoles (r=0.65). **D)** Model proposed for the bilateral modulation of
679 glomerular output in the olfactory bulb of *Xenopus* tadpoles. Juxtaglomerular neurons display
680 tonic dopamine release that inhibits glomerular output by activating presynaptic D2 receptors
681 present in OSNs (dotted box). The constant presence of dopamine within glomeruli is favored
682 by the activity of the contralateral olfactory bulb. When the contribution of the contralateral
683 pathway is suppressed, dopamine release diminishes, and glomerular responses become
684 potentiated. The contralateral modulation of the tonic activity of dopaminergic
685 juxtaglomerular neurons corrects for input differences and equalizes the synaptic output of
686 olfactory glomeruli to achieve a bilaterally balanced transfer of information. Axons sent by
687 mitral cells could mediate the pathway described but, the involvement of neurons found in

688 higher brain regions and participating in the processing of olfactory information, such as those
689 of the lateral pallium, could also be considered.
690

ACKNOWLEDGEMENTS

This work was sponsored by the Ministry of Science, Innovation and Universities (MICIU/AEI), grant PID2021-124536NB-I00 (A.L), co-funded by the European Regional Development Fund (ERDF), "a way of making Europe". The work was also supported by two Whitman Fellowships awarded to A.L in 2023 and 2024 (Marine Biological Laboratory, University of Chicago). The authors thank the institutional support from the María de Maeztu Unit of Excellence, Institute of Neurosciences, University of Barcelona, CEX2021-001159-M (Ministry of Science, Innovation and Universities) and the CERCA Program of Generalitat de Catalunya. A.L. is a Serra Húnter fellow.

REFERENCES

Banerjee, A., F. Marbach, F. Anselmi, M. S. Koh, M. B. Davis, P. Garcia da Silva, K. Delevich, H. K. Oyibo, P. Gupta, B. Li, and D. F. Albeanu. 2015. "An Interglomerular Circuit Gates Glomerular Output and Implements Gain Control in the Mouse Olfactory Bulb." *Neuron* 87 (1):193-207. doi: 10.1016/j.neuron.2015.06.019.

Belluscio, L., and L. C. Katz. 2001. "Symmetry, stereotypy, and topography of odorant representations in mouse olfactory bulbs." *J Neurosci* 21 (6):2113-22. doi: 10.1523/JNEUROSCI.21-06-02113.2001.

Boyd, J. D., and K. R. Delaney. 2002. "Tyrosine hydroxylase-immunoreactive interneurons in the olfactory bulb of the frogs Rana pipiens and Xenopus laevis." *J Comp Neurol* 454 (1):42-57. doi: 10.1002/cne.10428.

Browne, L. P., A. Crespo, and M. S. Grubb. 2022. "Rapid presynaptic maturation in naturally regenerating axons of the adult mouse olfactory nerve." *Cell Rep* 41 (10):111750. doi: 10.1016/j.celrep.2022.111750.

Byrd, C. A., and G. D. Burd. 1991. "Development of the olfactory bulb in the clawed frog, Xenopus laevis: a morphological and quantitative analysis." *J Comp Neurol* 314 (1):79-90. doi: 10.1002/cne.903140108.

Chaigneau, E., P. Tiret, J. Lecoq, M. Ducros, T. Knöpfel, and S. Charpak. 2007. "The relationship between blood flow and neuronal activity in the rodent olfactory bulb." *J Neurosci* 27 (24):6452-60. doi: 10.1523/JNEUROSCI.3141-06.2007.

Daume, D., T. Offner, T. Hassenklöver, and I. Manzini. 2022. "Patterns of." *Front Neuroanat* 16:914281. doi: 10.3389/fnana.2022.914281.

Ennis, M., F. M. Zhou, K. J. Ciombor, V. Aroniadou-Anderjaska, A. Hayar, E. Borrelli, L. A. Zimmer, F. Margolis, and M. T. Shipley. 2001. "Dopamine D2 receptor-mediated presynaptic inhibition of olfactory nerve terminals." *J Neurophysiol* 86 (6):2986-97. doi: 10.1152/jn.2001.86.6.2986.

Fino, E., R. Araya, D. S. Peterka, M. Salierno, R. Etchenique, and R. Yuste. 2009. "RuBi-Glutamate: Two-Photon and Visible-Light Photoactivation of Neurons and Dendritic spines." *Front Neural Circuits* 3:2. doi: 10.3389/neuro.04.002.2009.

Gaudin, A., and J. Gascuel. 2005. "3D atlas describing the ontogenic evolution of the primary olfactory projections in the olfactory bulb of Xenopus laevis." *J Comp Neurol* 489 (4):403-24. doi: 10.1002/cne.20655.

González, A., O. Marín, R. Tuinhof, and W. J. Smeets. 1994. "Ontogeny of catecholamine systems in the central nervous system of anuran amphibians: an immunohistochemical study with antibodies against tyrosine hydroxylase and dopamine." *J Comp Neurol* 346 (1):63-79. doi: 10.1002/cne.903460105.

Hayar, A., S. Karnup, M. Ennis, and M. T. Shipley. 2004. "External tufted cells: a major excitatory element that coordinates glomerular activity." *J Neurosci* 24 (30):6676-85. doi: 10.1523/JNEUROSCI.1367-04.2004.

Hill, R. A., E. C. Damisah, F. Chen, A. C. Kwan, and J. Grutzendler. 2017. "Targeted two-photon chemical apoptotic ablation of defined cell types in vivo." *Nat Commun* 8:15837. doi: 10.1038/ncomms15837.

Holl, A. M. 2018. "Survival of mature mouse olfactory sensory neurons labeled genetically perinatally." *Mol Cell Neurosci* 88:258-269. doi: 10.1016/j.mcn.2018.02.005.

Imamura, F., A. Ito, and B. J. LaFever. 2020. "Subpopulations of Projection Neurons in the Olfactory Bulb." *Front Neural Circuits* 14:561822. doi: 10.3389/fncir.2020.561822.

Kaneko, M., and T. Takahashi. 2004. "Presynaptic mechanism underlying cAMP-dependent synaptic potentiation." *J Neurosci* 24 (22):5202-8. doi: 10.1523/JNEUROSCI.0999-04.2004.

Karnup, S. V., A. Hayar, M. T. Shipley, and M. G. Kurnikova. 2006. "Spontaneous field potentials in the glomeruli of the olfactory bulb: the leading role of juxtaglomerular cells." *Neuroscience* 142 (1):203-21. doi: 10.1016/j.neuroscience.2006.05.068.

Kermen, F., P. Lal, N. G. Faturos, and E. Yaksi. 2020. "Interhemispheric connections between olfactory bulbs improve odor detection." *PLoS Biol* 18 (4):e3000701. doi: 10.1371/journal.pbio.3000701.

Kisilevsky, A. E., and G. W. Zamponi. 2008. "D2 dopamine receptors interact directly with N-type calcium channels and regulate channel surface expression levels." *Channels (Austin)* 2 (4):269-77. doi: 10.4161/chan.2.4.6402.

Kiyokage, E., Y. Z. Pan, Z. Shao, K. Kobayashi, G. Szabo, Y. Yanagawa, K. Obata, H. Okano, K. Toida, A. C. Puche, and M. T. Shipley. 2010. "Molecular identity of periglomerular and short axon cells." *J Neurosci* 30 (3):1185-96. doi: 10.1523/JNEUROSCI.3497-09.2010.

Kludt, E., C. Okom, A. Brinkmann, and D. Schild. 2015. "Integrating temperature with odor processing in the olfactory bulb." *J Neurosci* 35 (20):7892-902. doi: 10.1523/JNEUROSCI.0571-15.2015.

Lecoq, J., P. Tiret, and S. Charpak. 2009. "Peripheral adaptation codes for high odor concentration in glomeruli." *J Neurosci* 29 (10):3067-72. doi: 10.1523/JNEUROSCI.6187-08.2009.

Lodovichi, C. 2021. "Topographic organization in the olfactory bulb." *Cell Tissue Res* 383 (1):457-472. doi: 10.1007/s00441-020-03348-w.

Lodovichi, C., L. Belluscio, and L. C. Katz. 2003. "Functional topography of connections linking mirror-symmetric maps in the mouse olfactory bulb." *Neuron* 38 (2):265-76. doi: 10.1016/s0896-6273(03)00194-6.

Love, N. R., Y. Chen, S. Ishibashi, P. Kritsiligkou, R. Lea, Y. Koh, J. L. Gallop, K. Dorey, and E. Amaya. 2013. "Amputation-induced reactive oxygen species are required for successful Xenopus tadpole tail regeneration." *Nat Cell Biol* 15 (2):222-8. doi: 10.1038/ncb2659.

Manzini, I., C. Brase, T. W. Chen, and D. Schild. 2007. "Response profiles to amino acid odorants of olfactory glomeruli in larval Xenopus laevis." *J Physiol* 581 (Pt 2):567-79. doi: jphysiol.2007.130518 [pii]
10.1113/jphysiol.2007.130518.

Manzini, I., and D. Schild. 2004. "Classes and narrowing selectivity of olfactory receptor neurons of Xenopus laevis tadpoles." J *Gen Physiol* 123 (2):99-107. doi: jgp.200308970 [pii]
10.1085/jgp.200308970.

Manzini, I., D. Schild, and C. Di Natale. 2022. "Principles of odor coding in vertebrates and artificial chemosensory systems." Ph*ysiol Rev 1*02 (1):61-154. doi: 10.1152/physrev.00036.2020.

McGann, J. P. 2013. "Presynaptic inhibition of olfactory sensory neurons: new mechanisms and potential functions." Ch*em Senses 3*8 (6):459-74. doi: 10.1093/chemse/bjt018.

Menini, A. 2010. "The Neurobiology of Olfaction." In.

Mombaerts, P., F. Wang, C. Dulac, S. K. Chao, A. Nemes, M. Mendelsohn, J. Edmondson, and R. Axel. 1996. "Visualizing an olfactory sensory map." Ce*ll 8*7 (4):675-86. doi: 10.1016/s0092-8674(00)81387-2.

Moreno, N., R. Morona, J. M. López, L. Dominguez, M. Muñoz, and A. González. 2008. "Anuran olfactory bulb organization: embryology, neurochemistry and hodology." Br*ain Res Bull 7*5 (2-4):241-5. doi: 10.1016/j.brainresbull.2007.10.027.

Murphy, G. J., L. L. Glickfeld, Z. Balsen, and J. S. Isaacson. 2004. "Sensory neuron signaling to the brain: properties of transmitter release from olfactory nerve terminals." J *Neurosci 2*4 (12):3023-30. doi: 10.1523/JNEUROSCI.5745-03.2004.

Nezlin, L. P., and D. Schild. 2000. "Structure of the olfactory bulb in tadpoles of Xenopus laevis." Ce*ll Tissue Res 3*02 (1):21-9.

Niethammer, P., C. Grabher, A. T. Look, and T. J. Mitchison. 2009. "A tissue-scale gradient of hydrogen peroxide mediates rapid wound detection in zebrafish." Na*ture 4*59 (7249):996-9. doi: 10.1038/nature08119.

Nieuwkoop, P.D, and J. Faber. 1956. No*rmal table of Xenopus laevis (Daudin). A systematical and chronological survey of the development from the fertilized egg till the end of metamorphosis.:* Amsterdam: North-Holland Publishing Company. Guilders.

Petzold, GC, DF Albeanu, TF Sato, and VN Murthy. 2008. "Coupling of neural activity to blood flow in olfactory glomeruli is mediated by astrocytic pathways." Ne*uron 5*8 (6):897-910. doi: S0896-6273(08)00403-0 [pii]
10.1016/j.neuron.2008.04.029.

Pírez, N., and M. Wachowiak. 2008. "In vivo modulation of sensory input to the olfactory bulb by tonic and activity-dependent presynaptic inhibition of receptor neurons." J N*eurosci 28* (25):6360-71. doi: 10.1523/JNEUROSCI.0793-08.2008.

Shepherd, G.M., W.R. Chen, and C.A. Greer. 2004. The *Synaptic Organization of the Brain: O*xford University Press.

Terni, B., and A. Llobet. 2021. "Axon terminals control endolysosome diffusion to support synaptic remodelling." Lif*e Sci Alliance 4* (8). doi: 10.26508/lsa.202101105.

Terni, B., P. Pacciolla, H. Masanas, P. Gorostiza, and A. Llobet. 2017. "Tight temporal coupling between synaptic rewiring of olfactory glomeruli and the emergence of odor-guided behavior in Xenopus tadpoles." J C*omp Neurol 52*5 (17):3769-3783. doi: 10.1002/cne.24303.

Terni, B., P. Pacciolla, M. Perelló, and A. Llobet. 2018. "Functional Evaluation of Olfactory Pathways in Living Xenopus Tadpoles." J V*is Exp (1*42). doi: 10.3791/58028.

Wachowiak, M., and L. B. Cohen. 1999. "Presynaptic inhibition of primary olfactory afferents mediated by different mechanisms in lobster and turtle." J N*eurosci 19* (20):8808-17. doi: 10.1523/JNEUROSCI.19-20-08808.1999.

Wachowiak, M., J. P. McGann, P. M. Heyward, Z. Shao, A. C. Puche, and M. T. Shipley. 2005. "Inhibition [corrected] of olfactory receptor neuron input to olfactory bulb glomeruli mediated by suppression of presynaptic calcium influx." J N*europhysiol 94* (4):2700-12. doi: 10.1152/jn.00286.2005.

Weiss, J., M. Pyrski, P. Weissgerber, and F. Zufall. 2014. "Altered synaptic transmission at olfactory and vomeronasal nerve terminals in mice lacking N-type calcium channel Cav2.2." Eur *J Neurosci 40* (10):3422-35. doi: 10.1111/ejn.12713.

Weiss, L., I. Manzini, and T. Hassenklöver. 2021. "Olfaction across the water-air interface in anuran amphibians." Cel*l Tissue Res 38*3 (1):301-325. doi: 10.1007/s00441-020-03377-5.

Wu, Y., L. Dissing-Olesen, B. A. MacVicar, and B. Stevens. 2015. "Microglia: Dynamic Mediators of Synapse Development and Plasticity." Tre*nds Immunol 36* (10):605-613. doi: 10.1016/j.it.2015.08.008.

Figure 1

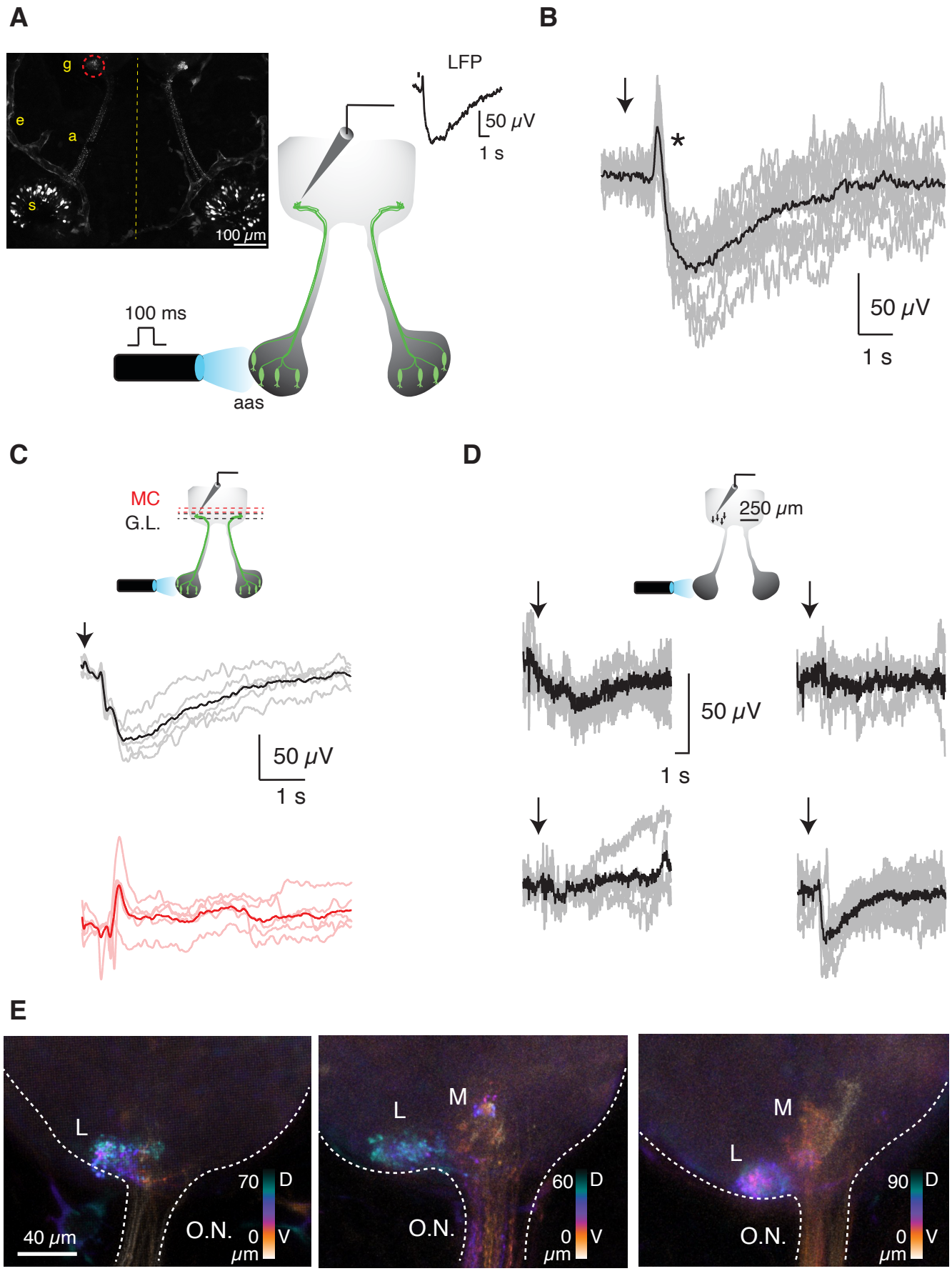
A
g
e
a
s
100 μm
LFP
50 μV
1 s
100 ms
aas
B
*
50 μV
1 s
C
MC
G.L.
50 μV
1 s
D
250 μm
50 μV
1 s
E
L
70
D
O.N.
0
V
μm
40 μm
L
M
60
D
O.N.
0
V
μm
M
L
90
D
O.N.
0
V
μm

Figure 2

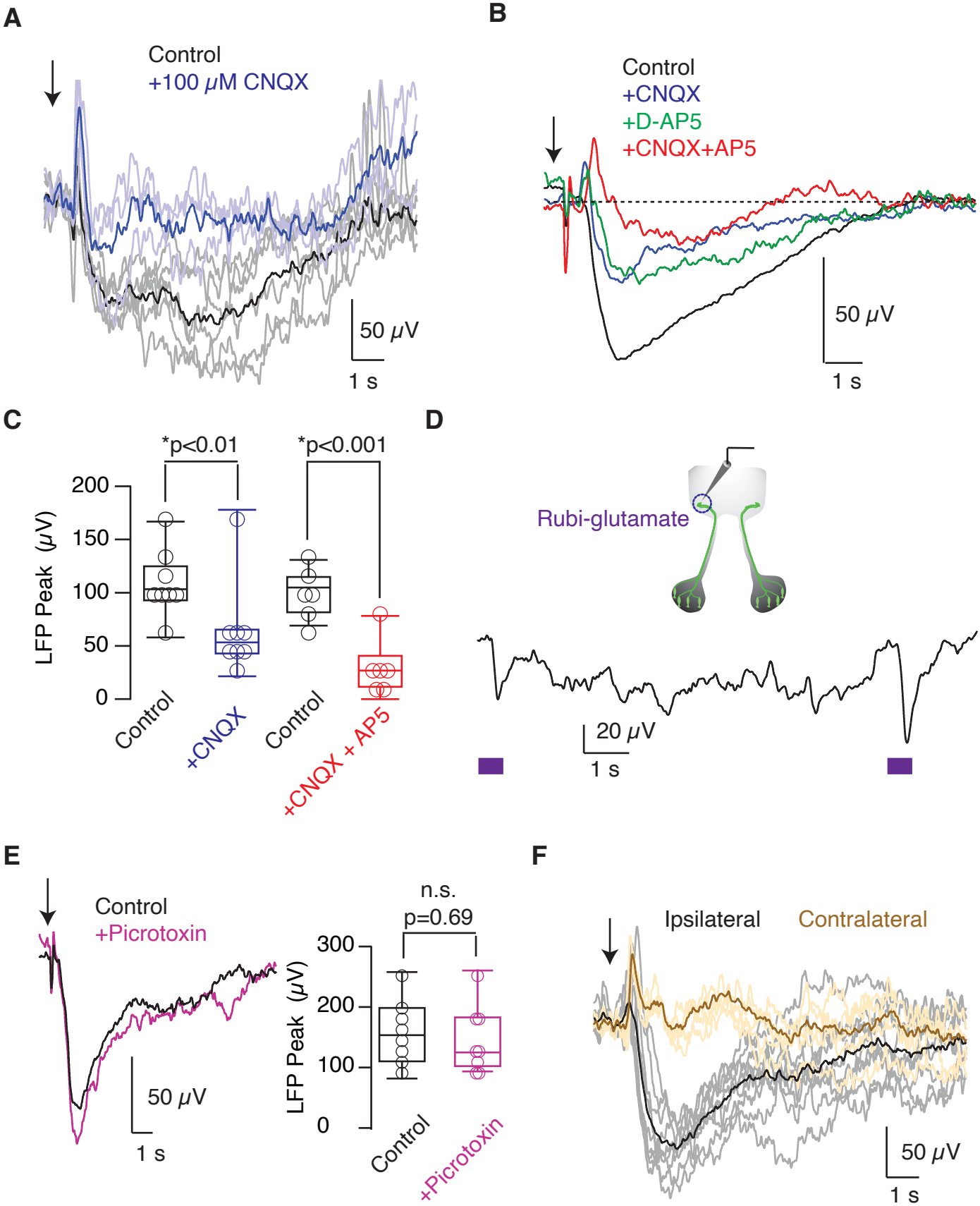
A
Control
+100 μM CNQX
50 μV
1 s
B
Control
+CNQX
+D-AP5
+CNQX+AP5
50 μV
1 s
C
*p<0.01
*p<0.001
LFP Peak (μV)
200
150
100
50
0
Control
+CNQX
Control
+CNQX + AP5
D
Rubi-glutamate
20 μV
1 s
E
Control
+Picrotoxin
50 μV
1 s
n.s.
p=0.69
LFP Peak (μV)
300
200
100
0
Control
+Picrotoxin
F
Ipsilateral
Contralateral
50 μV
1 s

Figure 3

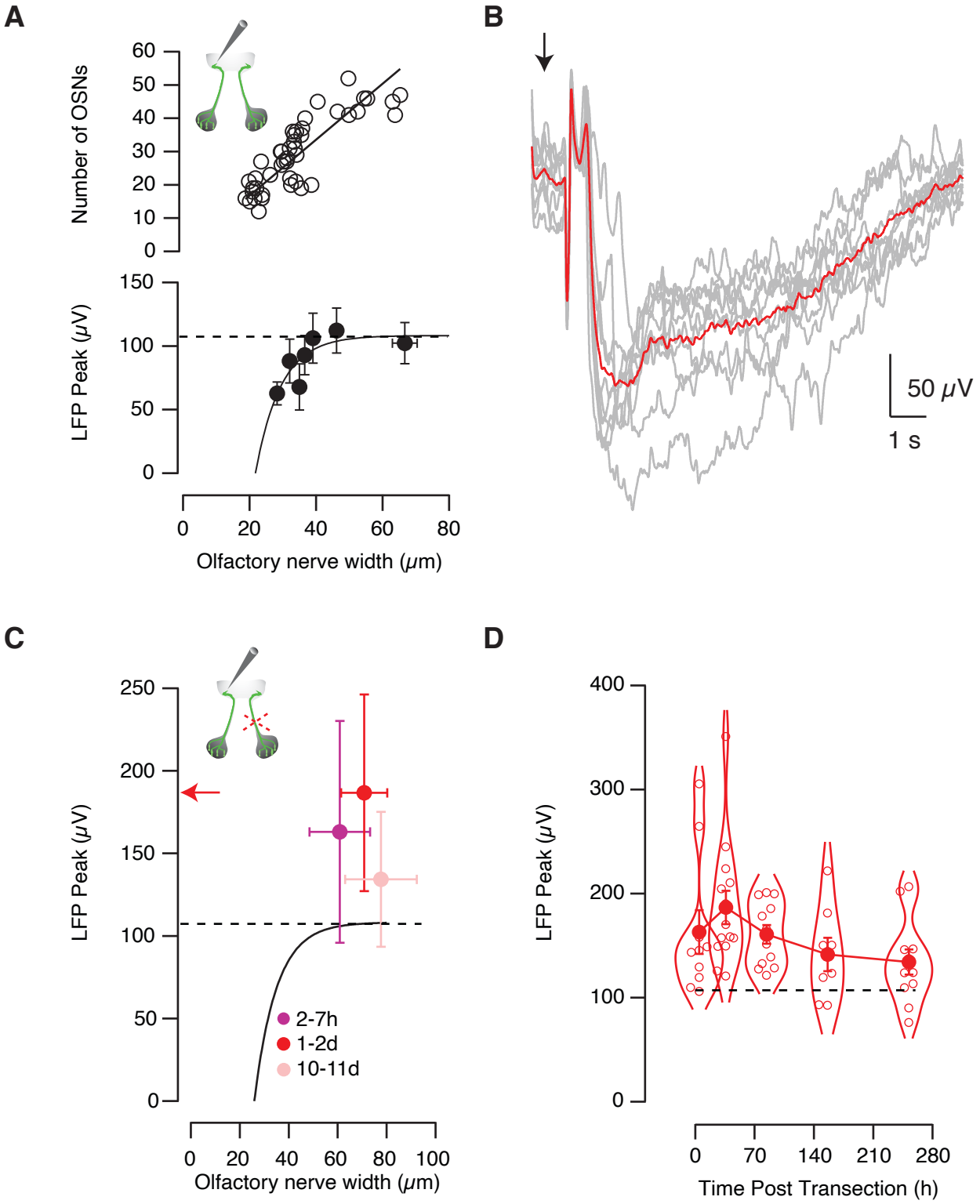
A
Number of OSNs
60
50
40
30
20
10
0
LFP Peak (μV)
150
100
50
0
0
20
40
60
80
Olfactory nerve width (μm)
B
50 μV
1 s
C
LFP Peak (μV)
250
200
150
100
50
0
2-7h
1-2d
10-11d
0
20
40
60
80
100
Olfactory nerve width (μm)
D
LFP Peak (μV)
400
300
200
100
0
0
70
140
210
280
Time Post Transection (h)

Figure 4

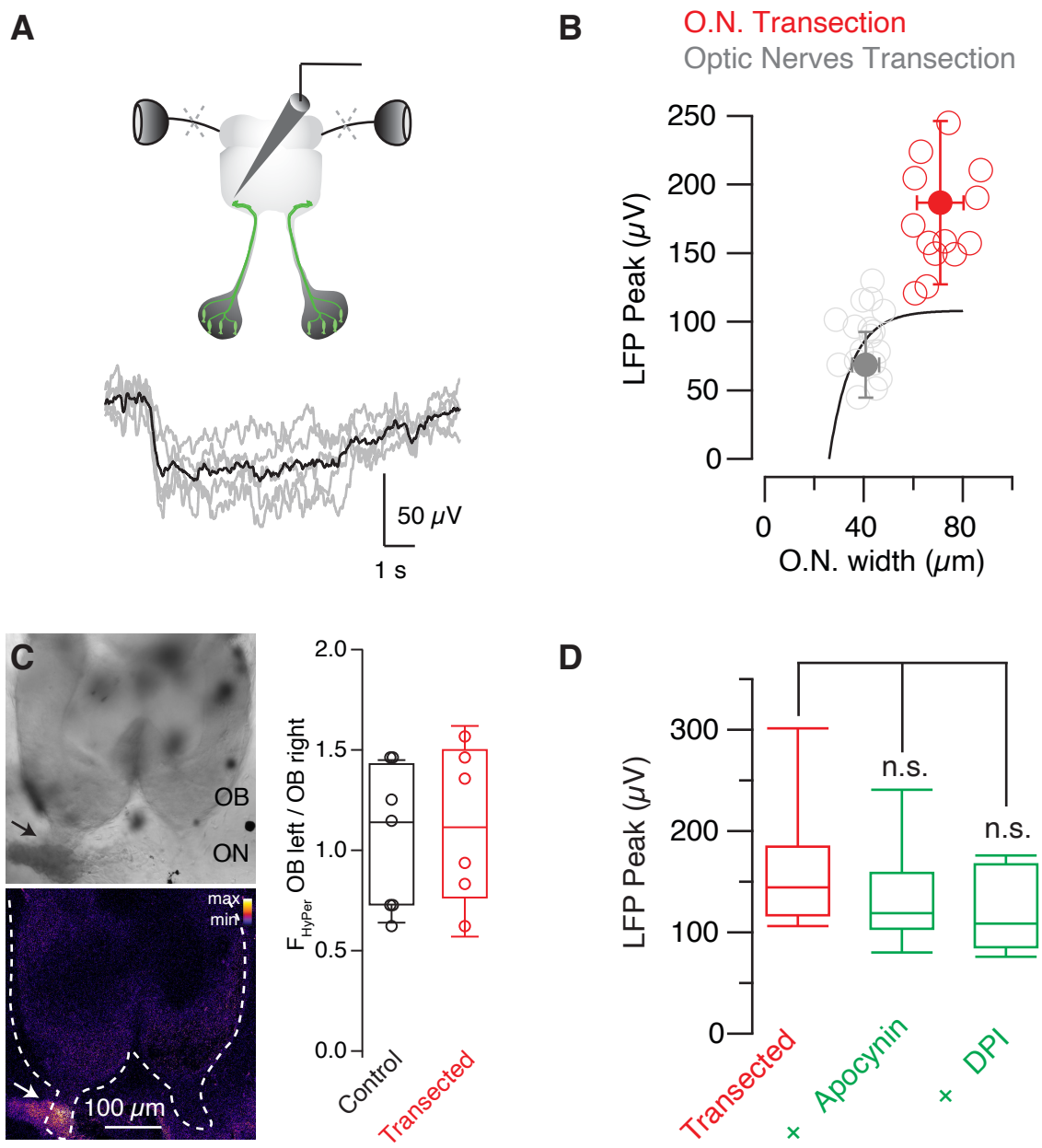
A
50 μV
1 s
B
O.N. Transection
Optic Nerves Transection
LFP Peak (μV)
250
200
150
100
50
0
0
40
80
O.N. width (μm)
C
OB
ON
max
min
100 μm
F HyPer OB left / OB right
2.0
1.5
1.0
0.5
0.0
Control
Transected
D
LFP Peak (μV)
300
200
100
0
n.s.
n.s.
Transected
+ Apocynin
+ DPI

Figure 5

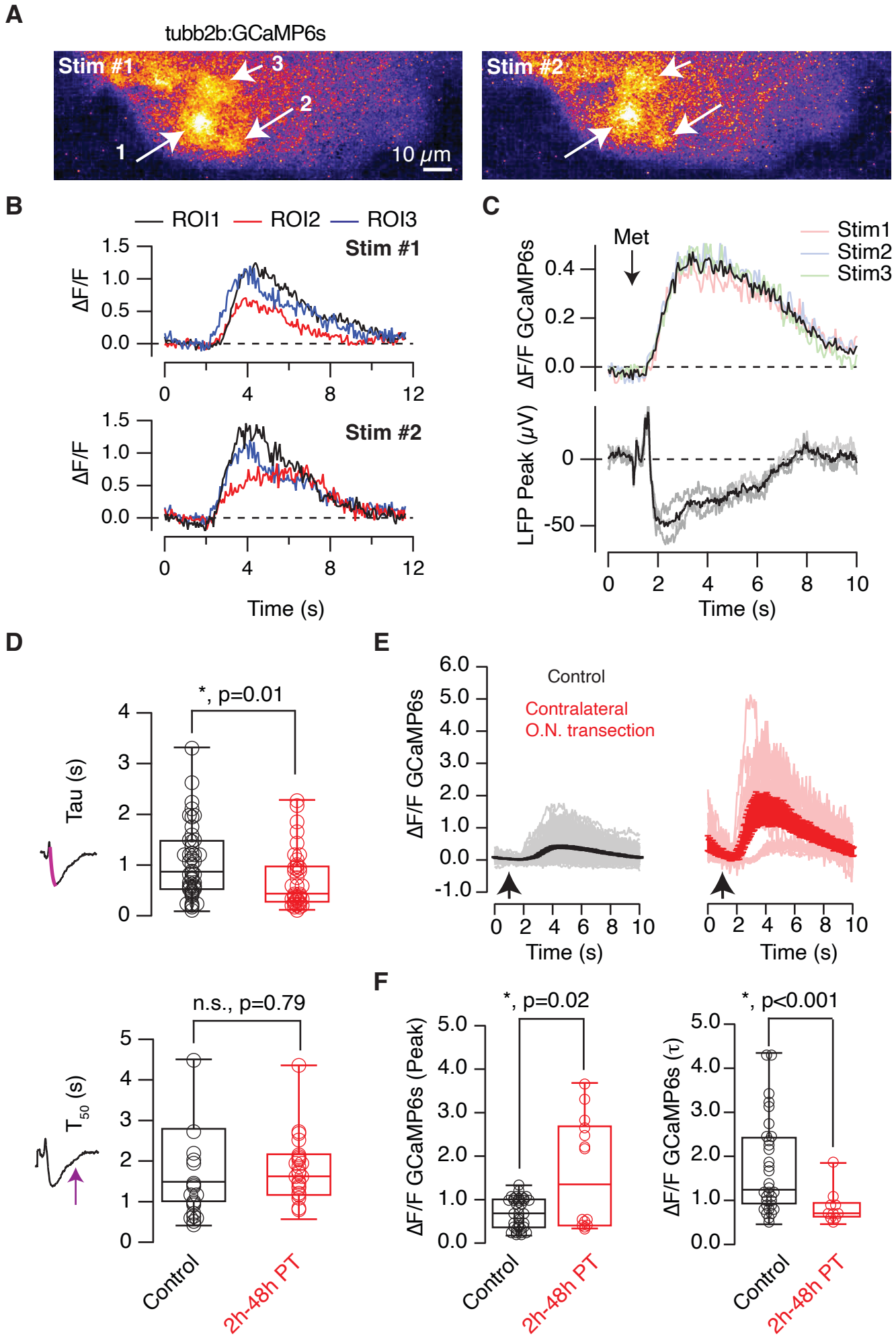
A
tubb2b:GCaMP6s
Stim #1
Stim #2
1
2
3
10 μm
B
ROI1
ROI2
ROI3
Stim #1
Stim #2
ΔF/F
Time (s)
C
Met
Stim1
Stim2
Stim3
ΔF/F GCaMP6s
LFP Peak (μV)
Time (s)
D
*, p=0.01
Tau (s)
E
Control
Contralateral
O.N. transection
ΔF/F GCaMP6s
Time (s)
F
n.s., p=0.79
T50 (s)
*, p=0.02
ΔF/F GCaMP6s (Peak)
*, p<0.001
ΔF/F GCaMP6s (τ)
Control
2h-48h PT

Figure 6

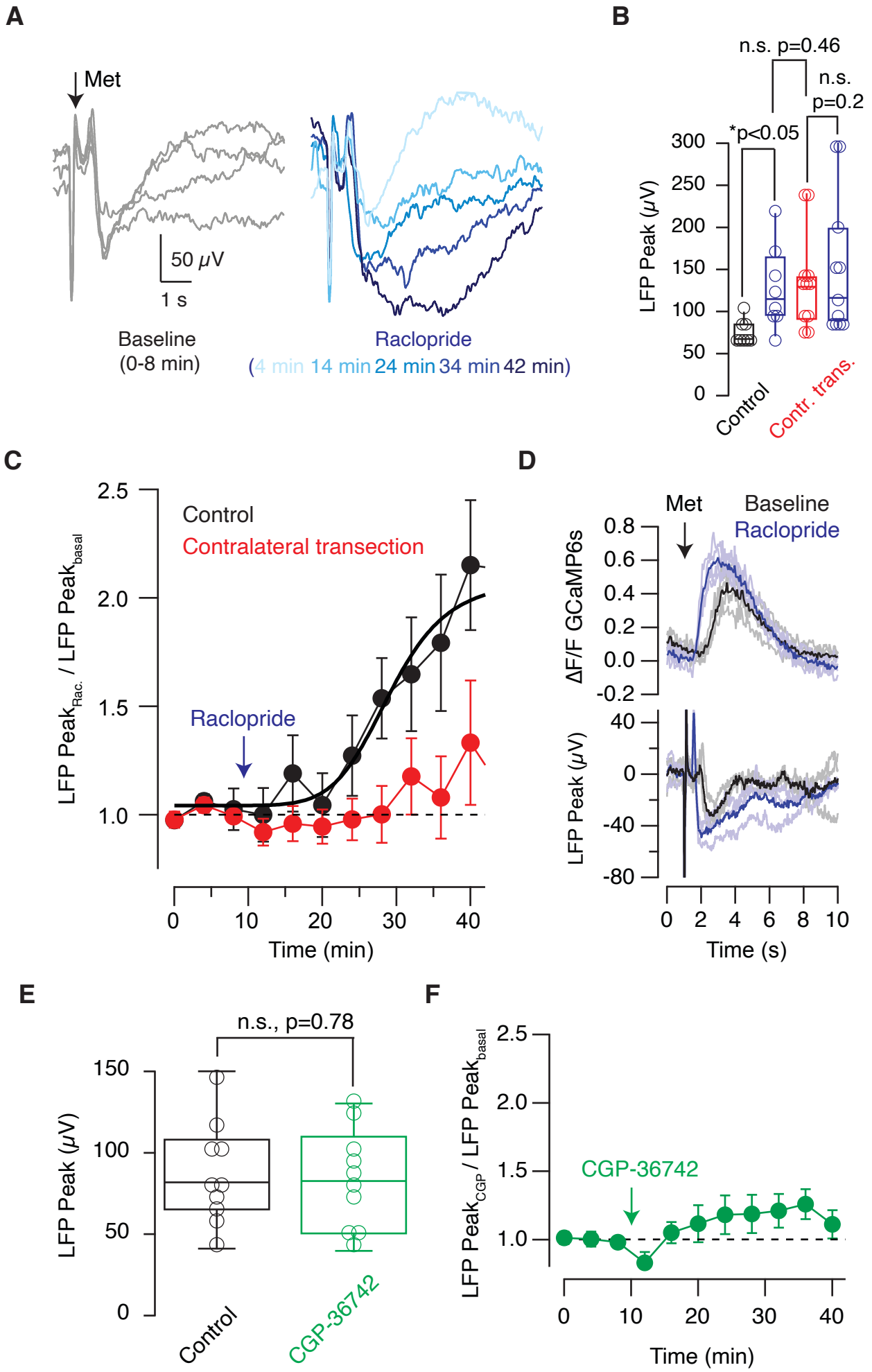
A
Met
50 μV
1 s
Baseline
(0-8 min)
Raclopride
(4 min 14 min 24 min 34 min 42 min)
B
n.s. p=0.46
n.s.
p=0.2
*p<0.05
LFP Peak (μV)
300
250
200
150
100
50
0
Control
Contr. trans.
C
Control
Contralateral transection
Raclopride
LFP Peak_Rac. / LFP Peak_basal
2.5
2.0
1.5
1.0
0
10
20
30
40
Time (min)
D
Met
Baseline
Raclopride
ΔF/F GCaMP6s
0.8
0.6
0.4
0.2
0.0
-0.2
LFP Peak (μV)
40
0
-40
-80
0
2
4
6
8
10
Time (s)
E
n.s., p=0.78
LFP Peak (μV)
150
100
50
0
Control
CGP-36742
F
CGP-36742
LFP Peak_CGP / LFP Peak_basal
2.5
2.0
1.5
1.0
0
10
20
30
40
Time (min)

Figure 7

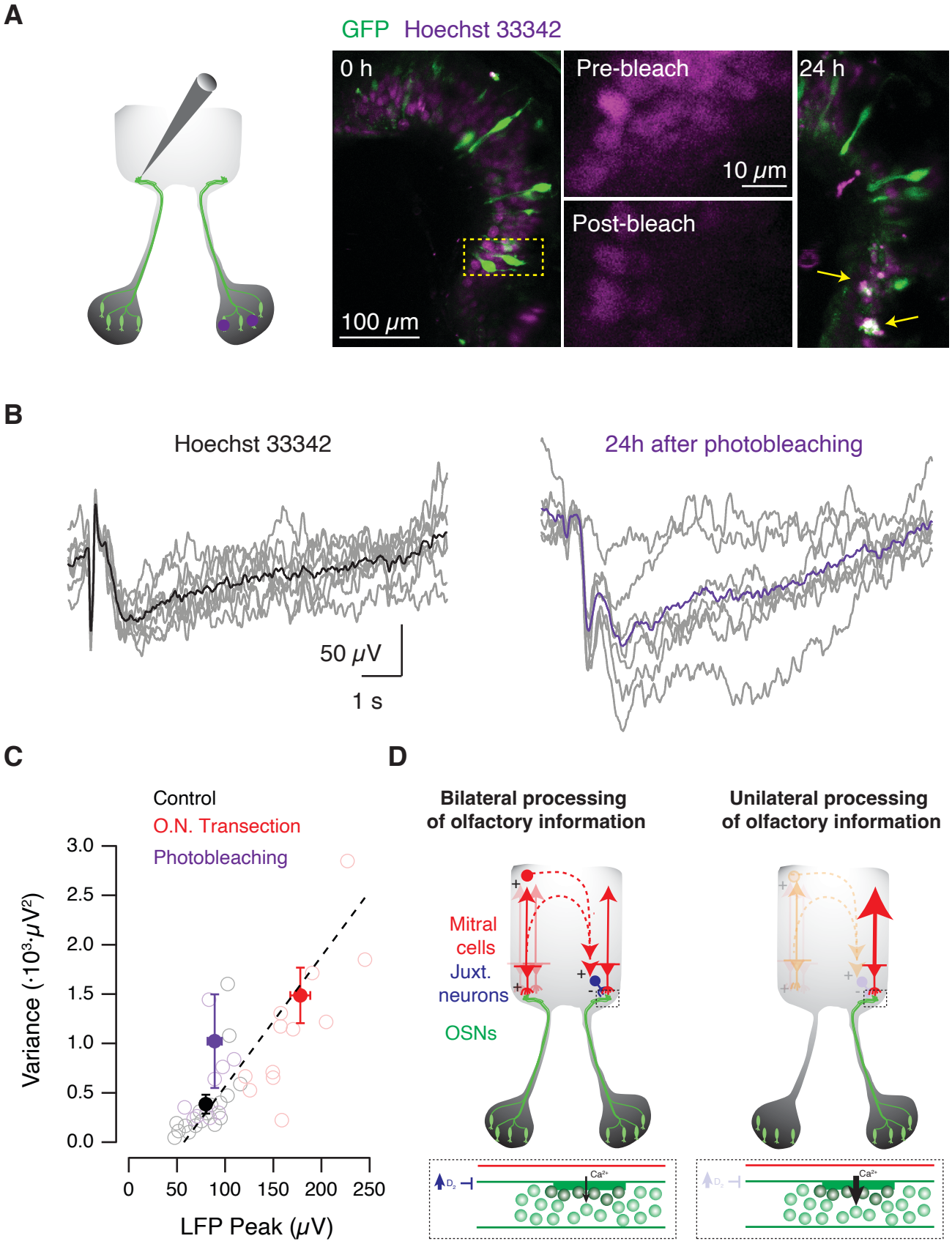
A
GFP Hoechst 33342
0 h
100 μm
Pre-bleach
10 μm
Post-bleach
24 h
B
Hoechst 33342
50 μV
1 s
24h after photobleaching
C
Control
O.N. Transection
Photobleaching
Variance (·10³·μV²)
3.0
2.5
2.0
1.5
1.0
0.5
0.0
0
50
100
150
200
250
LFP Peak (μV)
D
Bilateral processing of olfactory information
Unilateral processing of olfactory information
Mitral cells
Juxt. neurons
OSNs
Ca²⁺
Ca²⁺